# Analysis of Springback in Rotary Draw Bending Process: Numerical Modelling with Experimental Validation

*Rui.* L. Amaral[1,2*], *Daniel.* J. Cruz[1,2], *Maria* Almeida[2], *Manuel* Barros[3], *Abel* D. Santos[1,2], *Ana* Reis[1,2]

[1]Institute of Science and Innovation in Mechanical and Industrial Engineering (INEGI), Porto, Portugal
[2]Faculty of Engineering, University of Porto (FEUP), Porto, Portugal
[3]AMOB Group, Louro – V. N. Famalicão, Portugal

**Abstract.** Tubular components are widely used in aerospace and automotive industries due to their high strength, rigidity, energy absorption and light weight. Among tube bending techniques, Rotary Draw Bending (RDB) is the most industrially adopted due to its precision and versatility. However, elastic recovery after forming affects dimensional accuracy and must be carefully controlled. This phenomenon modifies the bent tube's angle and radius, impacting final part quality. This study models the RDB process using a simplified FEM to analyze key parameters, including bending angle, centerline radius, material thickness and their effect on elastic recovery. The model was validated through experiments with different testing parameters. Results demonstrated that an increase in bending angle doesn't significantly impact the elastic recovery radius but leads to an increase in the elastic recovery angle. Furthermore, an increase in the bend die radius leads to an increase in the elastic recovery radius and a decrease in the elastic recovery angle. The tube thickness doesn't significantly affect the elastic recovery radius or the elastic recovery angle for the studied material. Based on these findings, a predictive model was developed to support the design of industrial bending machines by correlating process variables with the tube geometry after elastic recovery.

**Keywords:** Rotary Draw Bending; Metal Forming; Springback; Finite Element Modelling

## 1 Introduction

Metal tube bending refers to the plastic forming processes that shape straight tubular profiles into complex geometries while preserving their cross-section. Formed tubes are essential in fluid conduction systems, structural components and decorative elements [1]. Their strength, rigidity and lightness make them valuable across industries, including agriculture, furniture, manufacturing, mobility (bicycle, automotive, naval, railway, aeronautical) and construction. Various bending techniques exist, such as three-point bending via manual or motorized presses, profile calendering and rotary bending with compression or stretching [2]. The choice of the most suitable process depends on factors such as thickness, diameter and application of the tube to be formed. Among these processes, rotary draw bending (RDB) offers a good compromise between precision and repeatability of the result, due above all to recent developments in tube bending machines. These innovations promote the transition from traditional hydraulic actuators to faster and more precise electric motors, increasing competitiveness in terms of productivity and efficiency [3].

As shown in Fig. 1, in this process the tube is stretched around a rotating tool that carries a clamp-die that restrains the tube against the bending tool. In addition, the pressure die follows the longitudinal movement of the tube, compensating for the bending moments during the bending operation. This technique is particularly used for bending thin-walled tubes, i.e. tubes with a low diameter/thickness ratio [4].

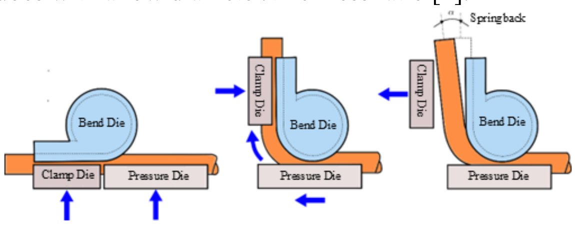


**Fig. 1.** Schematic of the rotary draw bending process.

In tube bending processes, especially for thinner tubes, it is common for defects to appear in the shape of the section, such as ovalisation, wrinkling or buckling on the internal surface. Another characteristic defect of this plastic forming method is a reduction in the thickness of the tube in the outer region of the bend, which in extreme cases can result in the material fracture.

Springback is a key factor in plastic forming, significantly affecting dimensional accuracy. After forming and die removal, the tube undergoes elastic recovery, altering the final bend angle and radius (Fig. 1). Predicting this effect is challenging due to its dependence on material elasto-plastic behaviour, tube geometry, process parameters and machine dynamics.

* Corresponding author: ramaral@inegi.up.pt

As shown in Fig. 2, in this article the geometry of the tube will be defined by the outer diameter (D), inner diameter (d) and wall thickness (t).

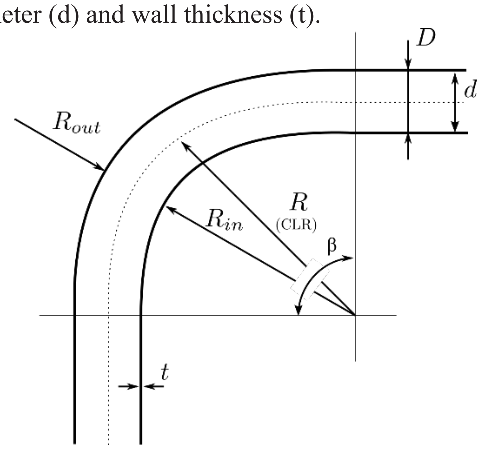


**Fig. 2.** Nomenclature used to describe the variables of the rotary draw bending process.

In addition, the bending geometry will be characterised by the inner ($R_{in}$) and outer ($R_{out}$) bending radii, or simply the average bending radius (CLR - Centre Line Radius). To facilitate the assessment and quantification of springback, its angle will be referred to as Δα and the radius as ΔCLR, which can be calculated using the following equations:

$$\Delta\alpha = |\alpha - \alpha_i| \quad (1)$$

$$\Delta CLR = |CLR - CLR_i| \quad (2)$$

where $CLR_i$ and CLR designate the radius of the central axis of the tube before and after removal of the clamping die, i.e. before and after elastic return, respectively. $\alpha_i$ and α designate the bending angles of the tube before and after removal of the clamping die, respectively.

Finally, the radius of the rotary bending tool will be defined by its average radius, $CLR_{BD}$.

Analytical and numerical approaches using finite element analysis (FEA) are commonly used to evaluate the behaviour of elastic response in bending process. These methods make it possible to reduce the time needed to design new products by eliminating steps in iterative experimental processes. Although analytical approaches often involve simplifications, they have the advantage of enabling rapid calculation of the elastic recovery and qualitative estimation of parameters effects.

Al-Qureshi and Russo [5] derived an analytical expression for the elastic-plastic behaviour in tube bending, showing that elastic-plastic boundary locations significantly affect the bending moment, springback, and residual stresses. However, their model assumes perfect plasticity, ignoring material hardening. Tang [6] developed a theoretical analysis of the forming behaviour in tube bending, considering ovalization, outer wall thinning and neutral layer displacement but also relied on perfect plasticity, limiting the accuracy. To refine analytical solutions, material hardening was later incorporated into models for neutral layer displacement, moment distribution, and springback analysis [7, 8].

The FEM is a useful tool for predicting process related defects. Gu et al. [9] analysed how geometry and material parameters affect the springback angle using a FE model that accounts for elasto-plastic behaviour. Their study showed that higher $CLR_{BD}$/D ratios increase the springback angle, while for small bending angles, reducing $CLR_{BD}$ and D leads to a rise in Δα. Fang et al. [10] used numerical simulation to examine geometric effects on springback angle of a titanium alloy, finding a linear relationship between bending angle and relative bending radius, unlike tube thickness and outer diameter. Da Xin et al. [11] studied tube bending with elastic feedback, accounting for material property variations. They found that Δα increases with the plasticity modulus (K), relative bending radius ($CLR_{BD}$/D) and bending angle (α) (though non-linearly) but decreases with the elasticity modulus (E), hardening coefficient (n) and thickness-to-diameter ratio (t/D). Li et al. [12] proposed a formulation to predict the final springback radius and bending angle change. Their numerical model showed ~5% error compared to experimental angular return and significant instability up to 100–120° of bend, stabilizing afterward.

This article aims to study the process of bending thick-walled tubes (t ≥ 5 mm) by rotary bending with stretching, with emphasis on quantifying the elastic return after plastic forming. The work will be carried out in three consecutive stages: (1) development of a parameterised finite element model capable of not only simulating the plastic forming of the tube during the rotary bending process, but also predicting the final geometry of the tube after springback; (2) investigating the impact of the main process parameters on the tube's springback, namely the bending angle (β), the bending matrix radius ($CLR_{BD}$), the tube thickness (t) and the tube diameter (D), through a parametric study; and (3) developing a predictive model capable of estimating the bending matrix radius ($CLR_{BD}$) required to achieve the desired final tube geometry after springback. This model will be essential for manufacturers of bending machines and tools, enabling them to avoid costly and time-consuming iterative processes that are often necessary to ensure that the final part achieves the desired CLR.

## 2 Materials

In this work, tubular profiles with different thicknesses made from S355J2 construction steel were analysed. This material is specified by the European standard EN 10025-2 and is widely used, especially in construction and other industrial applications that require high strength and toughness. To characterise the material mechanical behaviour, uniaxial tensile tests were carried out on specimens taken from tubes with a diameter of 114.3 mm and a thickness of 8 mm, following the ISO 16892 standard. The elasto-plastic behaviour of the material is described by Swift law:

$$\sigma_p = K\,(\varepsilon_p + \varepsilon_0)^n \quad (3)$$

The identified material properties and parameters are listed in Table 1.

**Table 1.** S355J2 materials properties.

| E [GPa] | YS [MPa] | UTS [MPa] | Swift Law | | |
|---|---|---|---|---|---|
| | | | $K$ [MPa] | $\varepsilon_0$ | $n$ |
| 198 | 420 | 567 | 928.7 | 0.0016 | 0.1659 |

## 3 Numerical Model

The finite element model for the rotary draw bending process was developed using the commercial software ABAQUS and validated using experimental tests. The numerical model is divided into two distinct phases.

In the first phase, the plastic deformation of the tube during the bending process is considered. The second phase analyses the elastic recovery of the tube after removing the bending tools. These two phases are modelled separately using different numerical formulations: an explicit non-linear approach for the forming and an implicit approach for the springback.

### 3.1 Plastic forming stage

In the first stage of the numerical model, several elements were considered: the bend die, characterised by its radius, $CLR_{BD}$, the pressure die, defined by its length, L, and the tube, defined by its diameter, D, and thickness, t.

Since the tools undergo less deformation than the tube, the bending and pressure dies were modelled as rigid analytical surfaces. The tube, however, was modelled as a deformable surface using S4R shell elements with reduced integration and five integration points. A convergence study determined an optimal mesh with 50 nodes around the perimeter and 140 along the length, totalling 7002 elements. The plastic forming model was based on an explicit nonlinear analysis. To minimize dynamic effects, the bend die rotated at 10 rad/s along the Oz axis, with a maximum bending angle (β) of 200°.

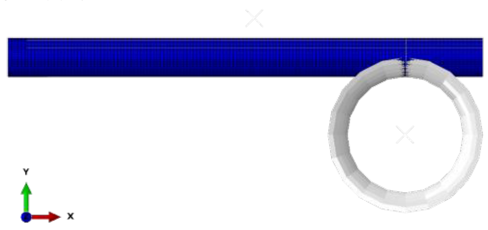

(a)

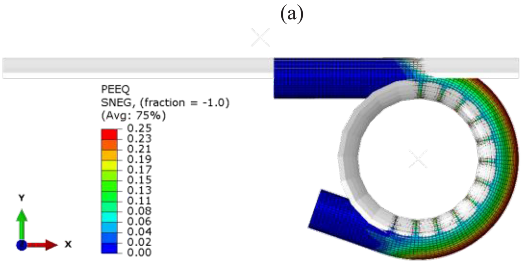


(b)

**Fig. 3.** Representation of the (a) numerical model of the plastic forming stage of the stretch rotary bending process and (b) distribution of the equivalent plastic deformation for a bending angle of 200° for S355J2 steel (D = 60.3 mm, t = 5 mm and $CLR_{BD}$ = 2D).

The contact between the tube and bend die was modelled with a friction coefficient of μ = 0.1, while the contact between the tube and the pressure die was defined with zero friction, since the pressure die follows the tube during the bending process and there is no relative movement between the surfaces.

Fig. 3 shows the numerical result for a bending angle β=200°, considering an S355J2 steel tube with a diameter of 60.3 mm, a thickness of 5 mm and a tool radius of $CLR_{BD}$=2D. It can be seen that the maximum equivalent plastic deformation imposed on the tube is approximately 25%.

### 3.2 Springback stage

Unlike the plastic forming stage, the springback stage used an implicit formulation for quasi-static problems. Here, only the tube was modelled, using the stress and strain distributions from bending as the initial state, without including tools or interactions. The only boundary condition applied was the restriction at one tube end. As noted in Section 1, springback is assessed through the springback angle (Δα) and radius (ΔCLR), given by Equations 1 and 2. Based on the plastic forming results, springback was evaluated at twenty intermediate stages between 10° and 200° of bending. Fig. 4 illustrates four stages at 10°, 90°, 140°, and 180°.

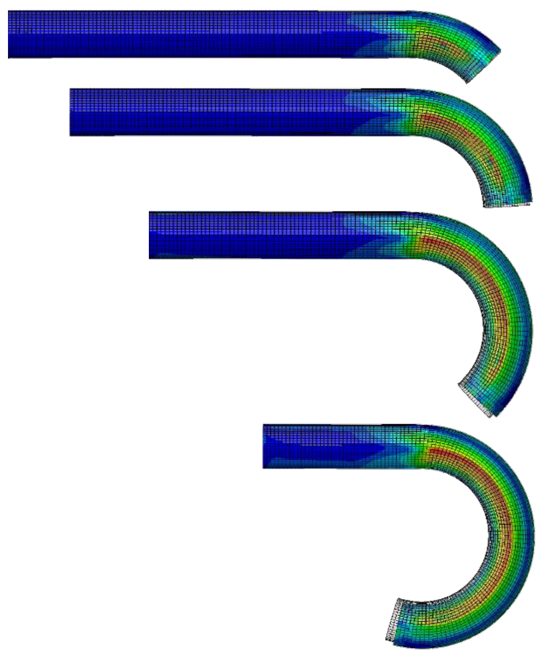

**Fig.4.** Representation of the tube geometry before and after springback for four bending stages with rotation angles β of 10º, 90º, 140º and 180º (from top to bottom).

For each stage, the tube's geometry before and after springback is presented, highlighting the differences, especially in later stages. Additionally, the equivalent stress distribution, based on the von Mises criterion, is shown on the bent surface. Once the springback model is completed, the springback angle and radius are determined for the twenty intermediate rotation angles.

### 3.3 Experimental Validation

In order to experimentally validate the finite element model developed, four case studies were selected using pipes made from the material S355J2. Table 2 summarises the pipe dimensions used (D, t, CLR). Experimentally, after bending, the tubes were measured using a digital 3D scanner, Hexagon Absolute Arm 83, in order to quantify the impact of springback on bending, Table 2 also summarises the results of all the case studies. The $CLR_{FEA}$ and $\alpha_{FEA}$ were obtained using the numerical model developed and represent the radius and elastic angle of return, respectively.

**Table 2.** Table summarising the pipe dimensions and results of numerical simulations.

| | Case1 | Case2 | Case3 | Case4 |
|---|---|---|---|---|
| D [mm] | 114.3 | 70.0 | 82.5 | 89.0 |
| t [mm] | 8.0 | 5.6 | 8.5 | 6.5 |
| $CLR_{BD}$ [mm] | 528 | 334 | 328 | 345 |
| $CLR_{Exp}$ [mm] | 542 | 349 | 337 | 343 |
| $CLR_{FEA}$ [mm] | 540 | 342 | 335 | 339 |
| Rel. error (CLR) [%] | 0.47 | 2.19 | 0.56 | 1.23 |
| $\alpha_{FEA}$ [º] | 179 | 178 | 177 | 177 |
| Rel. error (α) [%] | 0.62 | 1.11 | 1.66 | 1.61 |

The relative error for the radius was calculated using the experimentally measured $CLR_{Exp}$, while the bending angle error assumed an experimental angle of $\alpha = 180°$. The results indicate that the finite element model accurately predicts the CLR after springback, with a relative error below 3% in all cases. Notably, the experimental CLR after springback differs significantly from the tool radius, underscoring the relevance of the proposed methodology. The bending angle prediction ($\alpha_{FEA}$) performs even better, with a relative error below 2%. Despite some discrepancies, the four case studies validate the simulation, confirming its value as a predictive tool.

## 4 Predictive model for the geometry of bending tools

This section outlines the development of a predictive model to estimate the bend die radius ($CLR_{BD}$), incorporating the springback phenomenon and key parameters affecting tube behaviour. The model aims to accurately predict springback and will help speed up the process of designing bending tools, reducing time spent on iterative steps. A parametric analysis was conducted to evaluate the influence of various variables on tube springback, including tube diameter (D), thickness (t), bend die radius ($CLR_{BD}$) and bending angle (β). Numerical simulations were performed using the approach described in the previous section. Fig. 5 summarizes the combinations considered in the sensitivity analysis, which includes four tube diameters (60.3 mm, 70 mm, 114.3 mm, 139.7 mm), three thicknesses (5 mm, 8 mm, 10 mm) and five $CLR_{BD}$/D ratios (2, 2.5, 3, 4, 5). This test tree covers 60 combinations, with each simulation analysing a 200° bend in 10° increments, totalling 1260 simulations.

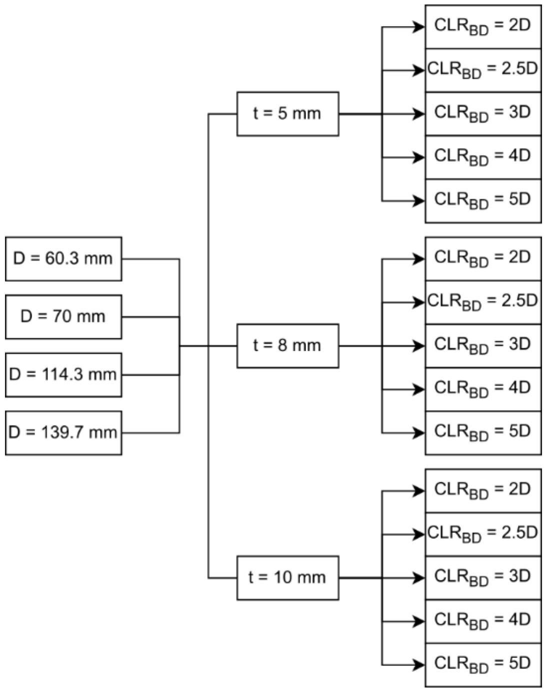


**Fig. 5.** Test tree combinations of simulated variables.

### 4.1 Influence of bending angle (β) on springback

This section evaluates the impact of bending angle on the springback radius (ΔCLR) and the corresponding springback angle (Δα). Fig. 6 shows this influence, using a tube with a diameter of D = 114.3 mm and thickness t = 8 mm, considering different $CLR_{BD}$/D ratios. As seen in Fig. 7a, the bending angle (β) has little effect on the springback radius, as it remains nearly constant for bending angles greater than 90º. Larger bend die radii result in larger springback radii. In contrast, the springback angle (Δα) is significantly affected by the bending angle (β), as shown in Fig. 6b. An increase in the bending angle amplifies the springback angle (Δα), while a reduction in $CLR_{BD}$ produces the same effect. Tighter bends induce greater strain gradients, increasing plastic deformation and, consequently, elastic recovery upon unloading, resulting in a more pronounced springback angle.

To generalize this parametric study, the impact of tube thickness on springback, both radius and angle, was evaluated. Three different thicknesses were tested for each combination of D and $CLR_{BD}$. Figures 7a and 7b show the evolution of the springback radius (ΔCLR) and springback angle (Δα), respectively, for a tube with D = 70 mm and $CLR_{BD}$/D = 2. The results indicate that tube thickness has no effect on the springback radius but does influence the springback angle. The lack of impact is reflected in Figure 7a, where the curves for different thickness values overlap, confirming that tube thickness does not significantly alter the overall response. Given this negligible effect, it is not necessary to include tube thickness as a variable in the predictive model formulation.

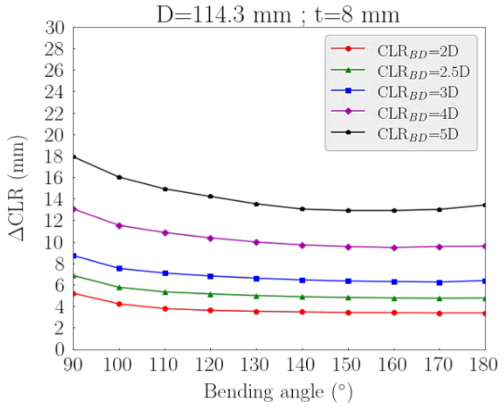

(a)

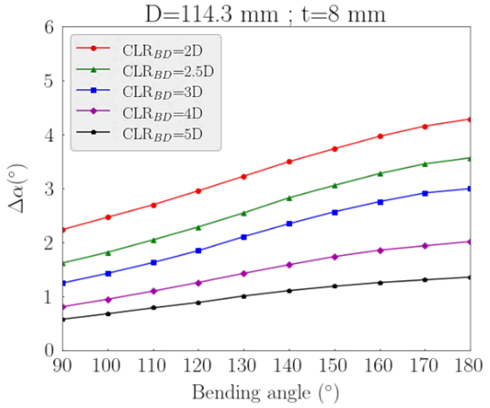

(b)

**Fig. 6.** Impact of bending angle (β) die radius (CLR$_{BD}$) on (a) springback radius, ΔCLR and (b) springback angle, Δα

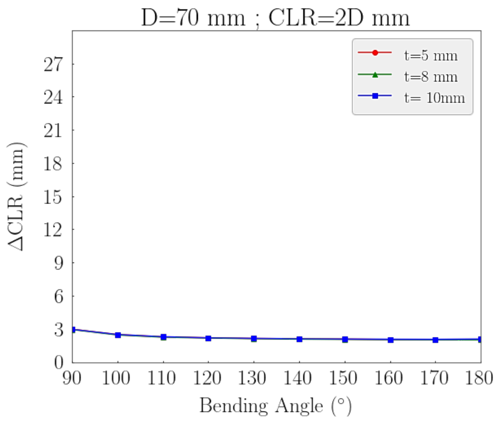

(a)

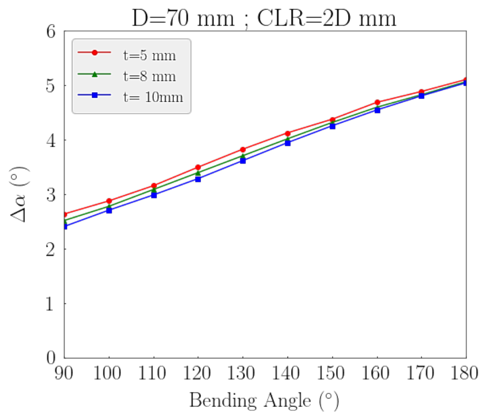

(b)

**Fig. 7.** Impact of bending angle (β) and tube thickness (t) on (a) springback radius, ΔCLR and (b) springback angle, Δα.

### 4.2 Influence of bend die radius on springback

This section presents the effect of the CLR$_{BD}$ radius on springback. This analysis enables the prediction of the appropriate CLR$_{BD}$ radius when designing the bend die, ensuring that the tube achieves the desired CLR after springback. Since the bending angle (β) has minimal impact on the springback radius, the following analysis considers a fixed bending angle of 180º.

Fig. 8 illustrates the evolution of springback, in terms of both radius and angle, as the CLR$_{BD}$/D ratio increases, considering tubes with different diameters but the same thickness (t = 8 mm). The results indicate that the ΔCLR increases with both the CLR$_{BD}$/D ratio and the tube diameter. Thus, for the same CLR$_{BD}$/D ratio, tubes with larger diameters exhibit higher springback radius. Conversely, the springback angle (Δα) follows an inverse trend, decreasing as both the CLR$_{BD}$/D ratio and tube diameter increase.

The predictive model developed must be able to estimate the required machining for CLR$_{BD}$ to achieve a tube with a specified CLR after a 180º bend. To reach this, it is essential to define the input and output parameters of the model. Given that tube thickness has a minimal impact on the springback of the material, particularly on the springback radius, the model will use the tube diameter and the desired CLR as input parameters, while the output parameter will be the required CLR$_{BD}$ for machining the bend die.

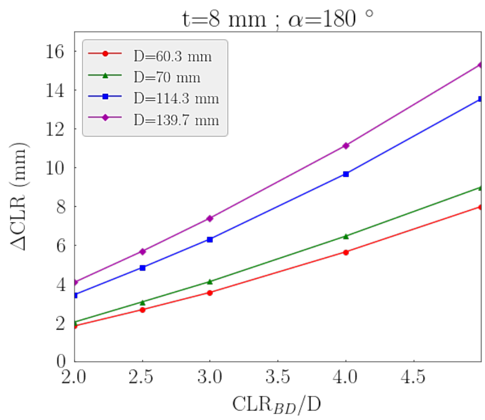

(a)

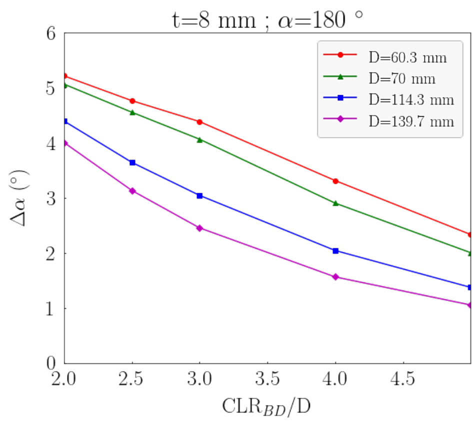

(b)

**Fig. 8.** Impact of CLR$_{BD}$/D ratio and tube diameter (D) on (a) springback radius, ΔCLR and (b) springback angle, Δα.

Different approaches were considered to define the input parameters, however, the most satisfactory results were achieved by considering, as input variables, the CLR/D ratio and the tube diameter, D:

$$CLR_{BD} = f(CLR/D, D) \tag{4}$$

To develop the predictive model, data from the combinations shown in Fig. 5 were used, excluding thicknesses other than t=5 mm, resulting in a total of 20 different combinations. To assess whether the output variables exhibit a clear trend or follow a specific relationship, a 3D representation was generated (Fig. 9), which correlates two input parameters (D and CLR/D) with the required $CLR_{BD}$. Additionally, discrete points from the case studies discussed earlier are included to validate the numerical model.

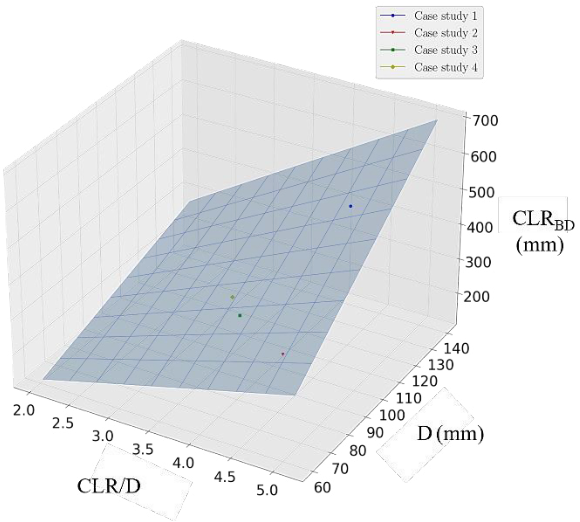


**Fig. 9.** 3D surface relating input parameters (D, CLR/D) to the bending tool diameter ($CLR_{BD}$).

Table 3 presents the comparison between the predicted $CLR_{BD}$ and the $CLR_{BD}$ used experimentally for the four case studies, all of which correspond to the experimental conditions listed in Table 2.

**Table 3.** Summary of experimental case studies.

| | | Case1 | Case2 | Case3 | Case4 |
|---|---|---|---|---|---|
| Input parameters | CLR/D | 4.74 | 4.99 | 4.09 | 3.86 |
| | D [mm] | 114.3 | 70 | 82.5 | 89 |
| $CLR_{BD}$ experimental | | 528 | 334 | 328 | 333 |
| $CLR_{BD}$ predicted | | 531 | 341 | 330 | 337 |
| Relative error | | 0.5% | 2.1% | 0.6% | 1.1% |

It can be observed that the predictive model accurately predicts $CLR_{BD}$, presenting very small relative errors, below 3%. It is also worth noting that the model overestimated the $CLR_{BD}$ for all case studies, which, despite the associated error, helps reduce the number of iterations required to produce bend dies, minimizing the risk of excessive machining. However, this model is limited to the material under study and also to the range of combinations considered.

## 5 Conclusions

This article aims to analyse the rotary draw bending of thick-walled tubes using a numerical approach, considering the springback phenomenon. A simplified FE model was developed and validated for S355J2 steel, showing relative errors under 3% in predicting both springback radius (ΔCLR) and angle (Δα). A sensitivity analysis identified the most influential variables in springback, considering tube diameters (D), thicknesses (t) and bend die radius ($CLR_{BD}$).

The parametric study shows that increasing the bending angle does not significantly affect ΔCLR but increases Δα. A larger $CLR_{BD}$ increases ΔCLR and decreases Δα, similar to the behaviour observed with the $CLR_{BD}$/D ratio. Tube thickness has minimal impact on ΔCLR or Δα. The numerical data led to the development of a highly accurate predictive model for estimating the $CLR_{BD}$ needed for a specific bending ratio CLR/D.

Future work could explore other materials to assess model robustness. Another path is integrating simplified mandrel and wiper tools to analyse wrinkles and ovalisation. Additionally, AI and machine learning could improve predictive models using numerical data, extending applicability to new conditions.

## Acknowledgements

The authors acknowledge the financial support from the FCT through LAETA under projects UIDB/50022/2020 and UIDP/50022/2020, as well as COMPETE2030-FEDER-01480000 project Smartubending. The second author acknowledges the financial support from FCT through the PhD scholarship 2022.12657.BD, granted under the POCH program and co-funded by the FSE and national funds from MCTES.

## References

1. S.A. Tronvoll, J. Ma, T. Welo, Int. J. Adv. Manuf. Technol. **124**, 801 (2023).
2. P. Martins, J. Rodrigues, Tecnologia da Deformação Plástica, Vol. II - Aplicações Industriais (Escolar Editora, 2010).
3. M. Strano, Int. J. Adv. Manuf. Technol. **26**, 733 (2005).
4. J. Gillanders, *Pipe & Tube Bending Manual* (Gulf Publishing Company, 1984).
5. H.A. Al-Qureshi, A. Russo, Mater. Eng. **23**, 217 (2002).
6. N.C. Tang, Int. J. Pressure Vessels Piping **77**, 751 (2000).
7. B. Engel, H.R. Hassan, Steel Res. Int. **85**, 1209 (2014).
8. D. Guan, J. Chen, J. Mater. Eng. Perform. **21**, 2316 (2012).
9. R.-J. Gu, H. Yang, M. Zhan, H. Li, Trans. Nonferrous Met. Soc. China **16**, s631 (2006).
10. J. Fang, S. Lu, K. Wang, C. Liang, X. Min, J. Phys. Conf. Ser. **1965**, 012107 (2021).
11. D.-x. E, H.-h. He, X.-y. Liu, R.-x. Ning, Int. J. Min. Metall. Mater. **16**, 177 (2009).
12. H. Li, H. Yang, F.F. Song, M. Zhan, G.J. Li, J. Mater. Process. Technol. **212**, 1973 (2012).